Journal of Cell Communication and Signaling (2022) 16:361–376
https://doi.org/10.1007/s12079-021-00665-9

RESEARCH ARTICLE

Connexin 32 overexpression increases proliferation, reduces gap junctional intercellular communication, motility and epithelial-to-mesenchymal transition in Hs578T breast cancer cells

Deniz Ugur[1,3] · Taha Bugra Gungul[1] · Simge Yucel[1] · Engin Ozcivici[2] · Ozden Yalcin-Ozuysal[1] · Gulistan Mese[1]

Received: 1 April 2021 / Accepted: 14 December 2021 / Published online: 4 July 2022

Abstract

Connexins (Cx) are primary components of gap junctions that selectively allow molecules to be exchanged between adjacent cells, regulating multiple cellular functions. Along with their channel forming functions, connexins play a variety of roles in different stages of tumorigenesis and their roles in tumor initiation and progression is isoform- and tissue-specific. While Cx26 and Cx43 were downregulated during breast tumorigenesis, Cx32 was accumulated in the cytoplasm of the cells in lymph node metastasis of breast cancers and Cx32 was further upregulated in metastasis. Cx32's effect on cell proliferation, gap junctional communication, hemichannel activity, cellular motility and epithelial-to-mesenchymal transition (EMT) were investigated by overexpressing Cx32 in Hs578T and MCF7 breast cancer cells. Additionally, the expression and localization of Cx26 and Cx43 upon Cx32 overexpression were examined by Western blot and immunostaining experiments, respectively. We observed that MCF7 cells had endogenous Cx32 while Hs578T cells did not and when Cx32 was overexpressed in these cells, it caused a significant increase in the percentages of Hs578T cells at the S phase in addition to increasing their proliferation. Further, while Cx32 overexpression did not induce hemichannel activity in either cell, it decreased gap junctional communication between Hs578T cells. Additionally, Cx32 was mainly observed in the cytoplasm in both cells, where it did not form gap junction plaques but Cx32 overexpression reduced Cx43 levels without affecting Cx26. Moreover, migration and invasion potentials of Hs578T and migration in MCF7 were reduced upon Cx32 overexpression. Finally, the protein level of mesenchymal marker N-cadherin decreased while epithelial marker ZO-1 and E-cadherin increased in Hs578T cells. We observed that Cx32 overexpression altered cell proliferation, communication, migration and EMT in Hs578T, suggesting a tumor suppressor role in these cells while it had minor effects on MCF7 cells.

Keywords Connexin 32 · Breast cancer · Proliferation · GJIC · Motility · EMT

Abbreviations

Cx	Connexin
GJIC	Gap junctional intercellular communication
GFP	Green fluorescent protein
CBX	Carbenoxolone
EMT	Epithelial-to-mesenchymal transition
MET	Mesenchymal-to-epithelial transition

✉ Gulistan Mese
gulistanmese@iyte.edu.tr

[1] Department of Molecular Biology and Genetics, Izmir Institute of Technology, Urla, Izmir 35430, Turkey

[2] Department of Bioengineering, Izmir Institute of Technology, Urla, Izmir, Turkey

[3] Department of Molecular Biology and Genetics, Avrasya University, Trabzon, Turkey

Background

Breast cancer constitutes 30% of all new cancer cases and is the second leading cause of cancer-related deaths among females (Siegel et al. 2020). Breast cancer has a high metastatic potential with 50% of patients having metastasis (Jin and Mu 2005). While the primary tumor is relatively benign, the cause of death is usually the metastasis of tumor cells to different tissues, primarily to the lungs, the bones, the brain and the liver (Weigelt et al. 2005). Several genetic and environmental factors including connexins (Cx) play roles

in tumorigenesis and metastasis of breast cancers (Ito et al. 2000; Kanczuga-Koda et al. 2006, 2007).

Cells in multicellular organisms continuously communicate with each other by different mechanisms, one of which is carried out by gap junctions. Gap junctions, formed from connexins (Cx) in chordates, allow the exchange of ions, secondary messengers and small metabolites between adjacent cells (Harris 2001). This intercellular communication is crucial for human physiology as alterations in connexins due to mutations, aberrant expression or localization that can impair connexin function and/or gap junctional intercellular communication (GJIC), can disrupt tissue homeostasis and lead to human disorders including cataracts, deafness and cancer (Paul 1995; Yamasaki et al. 1999; Sohl 2004; Cronier et al. 2009). There are 21 connexin isoforms in humans and the properties of channels are determined by the identities of the connexins forming the channel. Channels formed by different connexins serve distinct physiological functions as they have different gating properties, conductance and permeability, so the loss of one isoform cannot be compensated completely for by another one (Harris 2001; Willecke et al. 2002; Saez et al. 2003; Dahl and Muller, 2014).

Connexins are shown to have both tumor-promoting and tumor-suppressing functions (Unal et al. 2021). Re-introduction of connexins in GJIC-deficient cancer cells generally resulted in the reduction of cell proliferation, cell growth and tumor growth (Eghbali et al. 1991; Cronier et al. 2009). In addition, connexins altered cell cycle progression (Zhang et al. 2001; Sánchez-Alvarez et al. 2006; Burt et al. 2008), decreased tumor growth (Avanzo et al. 2004), angiogenesis and migration, supporting their tumor-suppressing functions (Qin et al. 2003; McLachlan et al. 2006). However, connexins are also associated with the invasiveness of tumor cells (Brauner and Hülser 1990; Li et al. 2007), where their expression promoted metastasis (Graeber and Hülser 1998; Ito et al. 2006). This dual nature of connexins with both tumorigenic and tumor suppressor roles is dependent on the isoform, cell/tissue type and cancer stage. One connexin can have diverse effects on different cancer cells. For example, Cx32 decreased proliferation in SKHep1 liver adenocarcinoma while it increased proliferation in Li7/Huh7 hepatocellular carcinomas (Li et al. 2007). In addition, different isoforms can have diverse effects on the same cell type. For instance, Cx32 decreased invasion while Cx43 increased it in HeLa cells, and Cx31 and Cx40 had no effect on the invasion of HeLa cervical cancer cells (Graeber and Hülser 1998).

Roles of Cx32 vary among various cancers. In Huh7 hepatocellular carcinoma cells, Cx32's effect is location-dependent as Cx32 mediated GJIC downregulated cell motility, while cytoplasmic Cx32 had a reverse effect (Li et al. 2007). This localization-dependent effect has also been observed in the prostate, gastric and colon cancers (Mehta 1999; Kanczuga-Koda et al. 2007; Jee et al. 2011). In the gastric carcinoma cell line AGS, re-localization of Cx32 from the plasma membrane to cytoplasm caused decreased Ki67 expression and its overexpression also resulted in cell cycle arrest at the G_1 phase by increasing the expression of p21Cip1 and p27Kip1 (Jee et al. 2013). Moreover, Cx32 transfection in lung carcinoma cell line A549 increased GJIC between cells and reduced the anchorage-independent growth, invasiveness and development of tumors in a xenograft model, while inducing contact inhibition (Hada 2006). Additionally, Cx32 promoted tube formation and migration in a hybrid of A549 lung cancer cells and HUVECs (EA.hy926) (Okamoto et al. 2014). These observations suggested that Cx32 influenced the cancer initiation and progression in a cell- and/or cancer-dependent manner.

In rodent breast tissue, Cx26, Cx32 and Cx43 are shown to be expressed (McLachlan et al. 2007). In humans, Cx26 and Cx43 are the major isoforms of the breast tissue where Cx26 is found in the breast epithelium and Cx43 is detected between myoepithelial cells of ducts (Monaghan et al. 1996). Recently, Cx32 was identified between luminal epithelial cells in the human breast (Teleki et al. 2014). In the initial phases of breast tumorigenesis, Cx26 and Cx43 are downregulated (Banerjee 2016) and when they were individually transfected into breast cancer cells, Cx26 and Cx43 functioned as tumor suppressors and restored the differentiation potential (Hirschi et al. 1996). Moreover, Cx26 and Cx43 also downregulated epithelial-to-mesenchymal transition (EMT) and upregulated molecular pathways linked to angiogenesis (McLachlan et al. 2006), supporting the tumor suppressor roles of Cx26 and Cx43 in breast cancers. During tumorigenesis, Cx32 was observed to be expressed in nearly 40% of invasive ductal breast cancers, and Cx32-negative primary tumors had Cx32-positive lymph-node metastases where Cx32 was mostly cytoplasmic (Kanczuga-Koda et al. 2007). Analysis of Cx32 in non-tumorigenic breast cells and invasive ductal breast cancer cells indicated its pro-tumorigenic roles (Adak et al. 2020). However, it is not clear if these roles were cell or stage-specific or dependent on Cx32 channel activities in breast cancers.

Cx32's GJIC-dependent, -independent and/or context-dependent functions in lung, liver and prostate cancers have been extensively studied but there is limited information about Cx32 in breast cancers. Inferred from Cx32's localization-dependent roles in other cancers and observation of cytoplasmic Cx32 in lymph-node metastasis, it was hypothesized that Cx32 might have localization-dependent functions in breast cancers. This study aimed to examine the role of Cx32 in MCF7 and Hs578T breast cancer cells examining its cellular localization, channel functions, association with other connexins, and tumor aggressiveness.

Material and methods

Cell culture

The human breast cancer cell lines MCF7 and Hs578T (ATCC) were cultured in high glucose Dulbecco's Modified Eagle Medium (DMEM, GIBCO, 41,966–029), supplemented with 10% fetal bovine serum (FBS, BI, 04–127-1A) and 1% penicillin/streptomycin (GIBCO, 15,140–122). 0.01 mg/mL insulin (Sigma, I1882) was added to the medium for Hs578T cells. All cells were maintained at 37°C and 5% CO_2 in a humidified atmosphere.

Both breast cancer cell lines were infected with Cx32 cloned into pLenti-GIII-CMV-GFP-2A-Puro lentiviral vector (ABMGOOD, LV169789) and its empty vector was used as a control. Viruses were produced in 293T cells by transfecting with lentiviral plasmid together with pMD2.VSVG envelope and pCMVdR8.74 packaging vectors as detailed in (Adak et al. 2020). After the titration in NIH3T3 cells, MCF7 and Hs587T cells were infected and selection with 2 µg/ml puromycin was started 72 h post-infection, and continued until all uninfected cells died.

For transient transfection, Cx32 gene was cloned into pCS2 + mammalian expression vector and empty vector were used as mock-transfection control. Cells were seeded 2×10^5 cells/well for Hs578T and 3×10^5 cells/well for MCF7 cells in 6-well plates and were transfected with FuGENE® (Promega, E2311) transfection reagent with 2 µg DNA: 3 µl transfection reagent ratio. After transfection, cells were incubated for 48 h until experimentation.

MCF7 and Hs578T cells were validated by using FTA Sample Collection Kit for Human Cell Authentication Service (ATCC, 135-XV). 1×10^6 cells/mL were prepared according to the manufacturer's instructions and sent to ATCC for STR analysis.

Cell counting and MTT analysis

For counting, cells were seeded at 5×10^4 cells/well for Hs578T and 1×10^5 cells/well for MCF7 in 6-well plates and were counted using a hemocytometer after trypan blue staining on days 1, 3 and 7 (GIBCO, 15250). For the MTT assay, cells were seeded at 2.5×10^3 cells/well for Hs578T and 5×10^3 cells/well for MCF7 in 12-well plates and were incubated with MTT (Amresco, 0793) for 4 h on the 1st, 3rd, 5th and 7th days. Then, crystals were dissolved in DMSO to measure the light absorbance of the samples at 570 nm.

Cell cycle analysis

Cells were trypsinized and centrifuged for 10 min at 1200 rpm at room temperature for flow cytometry analysis. Pellets were then resuspended with 1 ml cold PBS and 4 ml 100% ice-cold ethanol and kept at -20°C at least overnight. Before analysis, cells were treated with 0.1% Triton X-100 and 200 µg/ml RNase A (Sigma, R6148) in PBS. After the addition of 1 mg/ml PI solution (Life Technologies, T3605), cells were incubated for 15 min at dark. Cells were then analyzed by using BD FACS Canto flow cytometry.

Colony formation assay

Cells were seeded at 500 cells/well in 6-well plates for both cell lines and incubated for a week. Colonies formed after a week were fixed with 100% methanol for 20 min and washed with ddH_2O. Later, colonies were stained with 5% crystal violet (Amresco, 0528) for 10 min and washed three times with ddH_2O. Plates were then left to air-dry overnight. Images of the colonies within 78.5 mm^2 area were taken with bright field microscopy and colonies were counted.

Immunostaining

Cells were grown on glass coverslips for 2 days and were fixed with 4% paraformaldehyde (PFA) for 20 min, and permeabilized with 0.1%Triton-X for 15 min at room temperature. After blocking with 5% BSA for an hour, cells were incubated with primary antibody (1:200) for an hour and secondary antibody (1:200) and DAPI (Sigma, D95242) for 45 min. Antibodies used are as follows; rabbit anti-Cx32 primary antibody (Invitrogen, 345,700), rabbit anti-Cx43 primary antibody (Invitrogen, 710700), rabbit anti-Cx26 primary antibody (Invitrogen, 710500) and Alexa Fluor 555-conjugated anti-rabbit secondary antibody (Invitrogen, A21428). For colocalization experiments, cells were incubated with mouse anti-Golgin-97 primary antibody (Invitrogen, A21270), a Golgi apparatus marker together with rabbit anti-Cx32 primary antibody and washed with 1 × PBS. As a secondary antibody for Golgin-97, Alexa Fluor 488-conjugated anti-mouse antibody (Invitrogen, A11017) at 1:200 dilution was used.

For membrane staining, cells were incubated with Rhodamine conjugated-Wheat germ agglutinin (WGA, Vector Laboratories, RL-1022) in 1 × PBS at 1:500 dilution for 30 min at 4 °C and fixed with 4% PFA. The rest of the immunostaining protocol was followed afterward.

Scrape loading and dye-uptake assays

For scrape loading assay to determine gap junctional intercellular communication, after scrapes were made with a blade, cells were incubated with 0.5 mg/ml Neurobiotin (Vector Laboratories, 1120) for 10 min followed by a normal media incubation of 20 min. For dye uptake assay to investigate the hemichannel activity, cells were incubated with OPTI-MEM (Thermo Fisher, 31985070) for 20 min followed by Neurobiotin incubation for 10 min. For both assays, cells were later stained against Neurobiotin with rhodamine-conjugated streptavidin (Thermo Fisher, 21724) and DAPI. Blockage of hemichannels was achieved by using 100 µM Carbenoxolone (CBX). Cells were imaged using Olympus IX83 microscope and images were analyzed with ImageJ software (NIH). For the scrape loading assay, the distance travelled by Neurobiotin was calculated by a fitted curve, while for dye uptake assays amount of Neurobiotin was calculated by normalizing the signal received from the cells to the maximum signal.

Semi-quantitative RT-PCR analysis

Total RNA was isolated from fresh cells using Pure-link RNA Mini Kit (Invitrogen, 12183018A) according to the manufacturer's protocol. Then, complementary DNAs (cDNA) were synthesized from 1 µg total RNA by using Fermantas First Strand cDNA Synthesis Kit (Thermo Fisher, K1622). SYBR Green based qRT-PCR was performed in 96-well plates with 0.75 µl cDNA, 1 µl forward and reverse primers (100 µM), 2.25 µl dH_2O and 5 µl SYBR Green. The reaction was done in Roche LightCycler® 96. Primer sequences of the genes assessed are as follows: Cx26 F-5'-ctgcagctgatcttcgtgtc-3', Cx26 R-5'-aagcagtccacagtgttg-3', Cx32 F-5'-ggcacaaggtccacatct-3', Cx32 R-5'-gcatagccagggtagagc-3', Cx43 F-5'-gtgcctgaacttgccttttc-3', Cx43 R-5'-ccctcccagcagttgagtagg-3', GAPDH F-5'-gaaggtgaaggtcggagtca-3', GAPDH R-5'-aatgaaggggtcattgatgg-3'.

Western blot analysis

Total protein was isolated from fresh cells using lysis solution (10 mM Tris–HCl; 1 mM EDTA; 0.1% TritonX-100; 1% protease inhibitor; 0.1% DTT) and homogenizing with 26-gauge needle. Cells were centrifuged at 12,000 rpm for 20 min and the supernatant was collected. For subcellular fractionation for nuclear and cytoplasm extracts, proteins were isolated from fresh cells using a working solution (50 mM TrisHCl pH7.5; 150 mM NaCl; 10 mM NaF; 1% TritonX and 10 mM Imidazole in ddH_2O). Cells were incubated on ice for 5 min and centrifuged at 4°C and 14,000 rpm for 15 min. Supernatant was collected as cytoplasmic fraction and the pellet was washed with 1 × PBS and resuspended in working solution as nuclear fraction. For Western blotting, 15% resolving gels for connexins and 10% resolving gels for EMT markers together with 5% stacking gels were used. Equal amounts of proteins were incubated at 95°C for 5 min with 5 µl loading dye (250 mM Tris-HCI, 10% SDS, 30% Glycerol, 5% β-mercaptoethanol, 0.02% Bromophenol Blue). Samples were transferred to a nitrocellulose membrane. The membrane was blocked for 2 h with 5% milk in 1 × Tris-buffered Saline and Tween 20 (TBS-T) solution. The membrane was then incubated with proper primary antibody at 1:1000 dilution within 5% milk in TBS-T solution overnight at 4°C. On the following day, the membrane was incubated with 1:1000 dilution of respective secondary antibodies for 2 h at room temperature. The image was taken with SuperSignal® West Pico Chemiluminescent Substrate Detection Kit (Thermo Fisher, 34077). For loading control, mouse anti-γ-tubulin primary (Sigma, T6557) antibody at 1:1000 dilution and HRP-conjugated anti-mouse secondary antibody (Dako, P0447) at 1:1000 dilution was used. Protein levels were normalized to γ-tubulin using ImageJ software. The following antibodies were used for EMT markers: Snai1 (Cell Signaling, 3879P), E-Cadherin (Cell Signaling, 3195P), N-Cadherin (Cell Signaling, 13116P), and ZO-1 (Cell Signaling, 8193P).

Wound healing assay

Cells were seeded in 12 well plates at 9×10^5 cells/well for MCF7 and 4.5×10^5 cells/well for Hs578T. After 48 h incubation, 10 µg/ml mitomycin was added in serum-free medium for 2 h, and a wound was created with a 10 µl pipette tip. Afterward, cells were incubated in 1% serum-containing starvation medium for 18 h. During incubation, pictures were taken every hour using a Leica DMI8 confocal microscope equipped with an incubation chamber. The percentage of the open area was determined by using ImageJ software.

Invasion assay

Inserts (SPL, 37224) were coated with a 1:6 dilution of Matrigel in serum-free medium. Cells were seeded on the Matrigel at 5×10^4 cells/well for MCF7 and 7.5×10^4 cells/well for Hs578T in serum free medium, and inserts were incubated in normal medium for 18–24 h and then invading cells on the insert membrane were stained with DAPI. Images of the whole insert were taken by Olympus IX83 fluorescence microscope and were merged in cellSens program.

Soft agar analysis

1.5 ml of 0.5% agar (Difco, 214220) in medium was placed at the bottom of 6-well plates. After polymerization, 1.5 ml

of 0.35% agar containing 3×10^4 cells were placed on top of the 0.5% agar with 0.5 ml medium as the top layer. The medium was changed once a week until colonies of proper sizes (diameter > 30 µm) developed. For imaging, colonies were stained with 0.05% crystal violet and 5 stacks of 25 frames placed in a 5 × 5 grid were taken using a Leica confocal microscope. The images were analyzed using ImageJ software.

Statistical analysis

All data were expressed as mean ± standard deviation (S.D.) of at least three independent experiments. Significant differences were analyzed by comparing the data of GFP control with Cx32-infected cells and were indicated as statistically significant for $p < 0.05$ (*), $p < 0.01$ (**), $p < 0.005$ (***) and $p < 0.001$ (****) using Student's t-test.

Results

Determination of Cx32 expression in Hs578T and MCF7 cells

Although Cx32 was shown to be expressed in breast cancer tissues, its presence in Hs578T and MCF7 cell lines was previously not known. To assess the effects of Cx32 in these cells, the expression of Cx32 was determined at mRNA and protein levels using semi-quantitative RT-PCR and Western blotting, respectively. MCF7 cells had 55 times ($p < 0.001$) more Cx32 mRNA expression than Hs578T cells (Fig. 1A). Additionally, the presence of Cx32 protein was verified with Western blot in MCF7 cells, where there was a negligible amount of Cx32 protein in Hs578T cells while MCF7 cells had ~ 5 times ($p < 0.001$) more Cx32 protein compared to Hs578T cells (Fig. 1B). Moreover, the presence and localization of Cx32 fluorescent staining were consistent with mRNA and protein data, indicating limited Cx32 presence in Hs578T cells and a substantial amount of Cx32 in MCF7 cells (Fig. 1C). Even though MCF7 cells had endogenous Cx32, they did not show any gap junctional plaque formation at the cell–cell contact sites (Fig. 1C).

To investigate the effects of Cx32 overexpression in breast cancer cells, stable cell lines were generated by infecting Hs578T and MCF7 with GFP control and Cx32 lentiviruses (used as Hs578T-GFP, Hs578T-Cx32, MCF7-GFP and MCF7-Cx32 in the following parts) followed by puromycin antibiotic selection. Cx32 expression increased 274-fold in Hs578T cells and 180-fold in MCF7 cells at mRNA levels compared to control GFP cells (Fig. 2A). In addition, Cx32 protein level increased around 8-fold in Hs578T cells but did not change in MCF7 cells upon Cx32 overexpression (Fig. 2B).

Cx32 resulted in increased proliferation especially in Hs578T cells

Altered expression of connexins can interfere with the growth pattern of the cells through affecting viability and/or proliferation, so to assess the effects of Cx32 on growth curve, MTT analysis was conducted on days 1, 3, 5 and 7. Compared to Hs578T-GFP cells, Hs578T-Cx32 cells

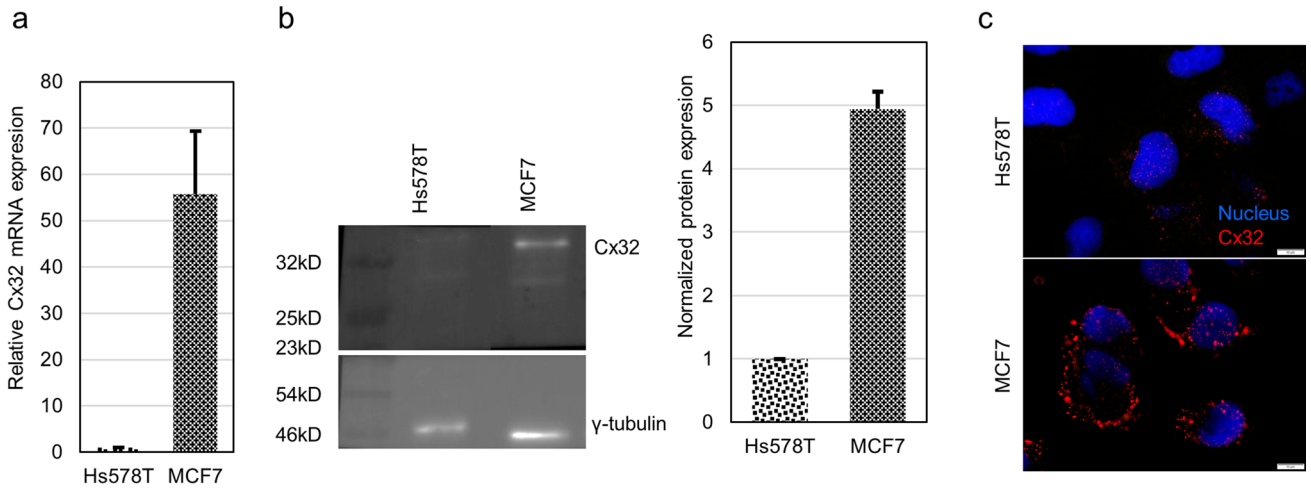

Fig. 1 MCF7 cells had endogenous Cx32 while Hs578T cells have a negligible amount of Cx32. Cx32 expression in Hs578T cells was normalized to 1 and Cx32 expression in MCF7 cells was compared to Cx32 expression in Hs578T cells at **a** mRNA levels of cells (n = 3). **b** Representative Western blot image of Cx32 protein levels in cells and quantification of protein levels in cells where Cx32 protein level was normalized to γ-tubulin levels (n = 3). **c** Localization of Cx32 protein in the cells. Red is Cx32 and blue is for the nucleus. The scale bar is 10 µm

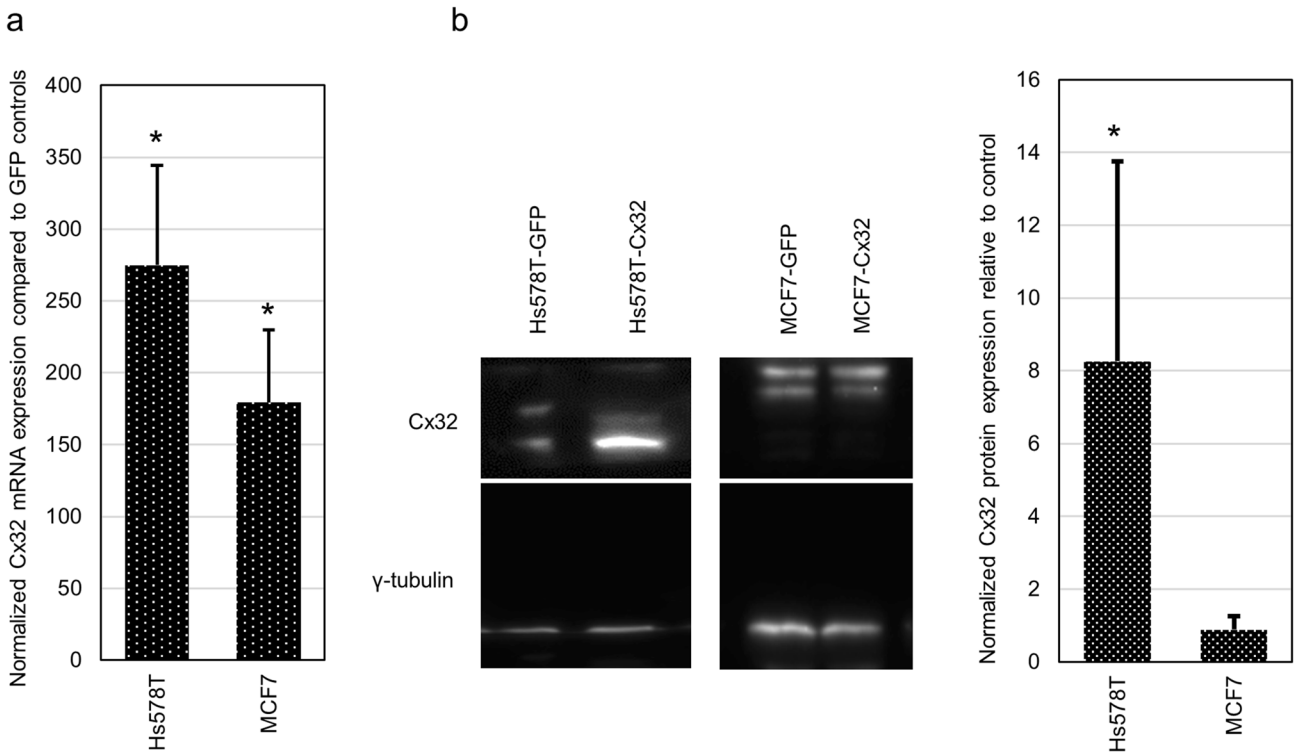

Fig. 2 Cx32 infection resulted in Cx32 overexpression in Hs578T cells at both mRNA and protein levels. Cx32 expression was compared by normalizing expression in Cx32 infected cells to control GFP cells **a** at mRNA levels in infected cells. (n = 3, $*p < 0.05$). **b** Representative image of Cx32 protein levels in infected cells, and quantitative comparison of protein levels in infected cells (n = 3, $*p < 0.05$). Error bars represent S.D

had 44% ($p < 0.05$), 40% ($p < 0.05$) and 57% ($p < 0.001$) more MTT signal on day 3, day 5 and day 7, respectively (Fig. 3A). In MCF7 cells, Cx32 infected cells also had higher MTT signal compared to GFP control cells, but the increase was only statistically significant on day 7 with a 47% increase in MCF7-Cx32 condition ($p < 0.05$) (Fig S1A). Proliferation was further assessed with cell counting using trypan blue staining and hemocytometer on days 1, 3, and 7 after culturing. Consistent with MTT analysis, Cx32 infected cells had a 34% increase in cell number compared to GFP infected counterparts on day 7 in Hs578T cells ($p < 0.05$, Fig. 3B). On the other hand, cell counting did not reveal any statistically significant change between GFP and Cx32 infected MCF7 cells (Fig S1B).

To investigate if the alteration in cell viability and/or proliferation in Hs578T cells was due to changes in cell cycle progression upon Cx32 overexpression, cell cycle analysis with PI staining and flow cytometry was conducted. The percentage of cells in the G_1 phase decreased significantly from 63% in Hs578T-GFP cells to 54% in Hs578T-Cx32 cells ($p < 0.05$) and in parallel with this decrease, the percentage of cells in the S phase significantly increased from 19.7% in Hs578T-GFP cells to 30.9% ($p < 0.001$) in Hs578T-Cx32 with no significant change in G_2 phase. On the other hand, no changes were observed in the percentages of MCF7 cells in G_1, S or G_2 phases (Fig. 3C).

Finally, the survival and growth potential of cells were examined with the colony formation assay. Colony numbers increased ~1.6 fold in Hs578T-Cx32 compared to Hs578T-GFP cells ($p < 0.05$). Similarly, there was a 2.2 fold increase in the number of colonies formed by MCF7-Cx32 cells compared to MCF7-GFP cells but this increase was not statistically significant ($p = 0.13$, Fig. 3D).

Cx32 reduced GJIC between Hs578T cells without influencing hemichannel activity

Scrape-loading and dye uptake assays were performed to investigate the involvement of Cx32 gap junction channel and hemichannel activities in the proliferation of Hs578T cells upon Cx32 overexpression, respectively. Further, we used carbenoxolone to block hemichannel and gap junction channel activities in cells. For the gap junctional communication between cells, the distance of Neurobiotin transfer from the site of the scrape demonstrated that Hs578T cells were able to transfer the tracer from the site of the scrape to neighboring cells, indicating GJIC between cells (Fig. 4A). While GFP control cells had the highest level of dye transfer

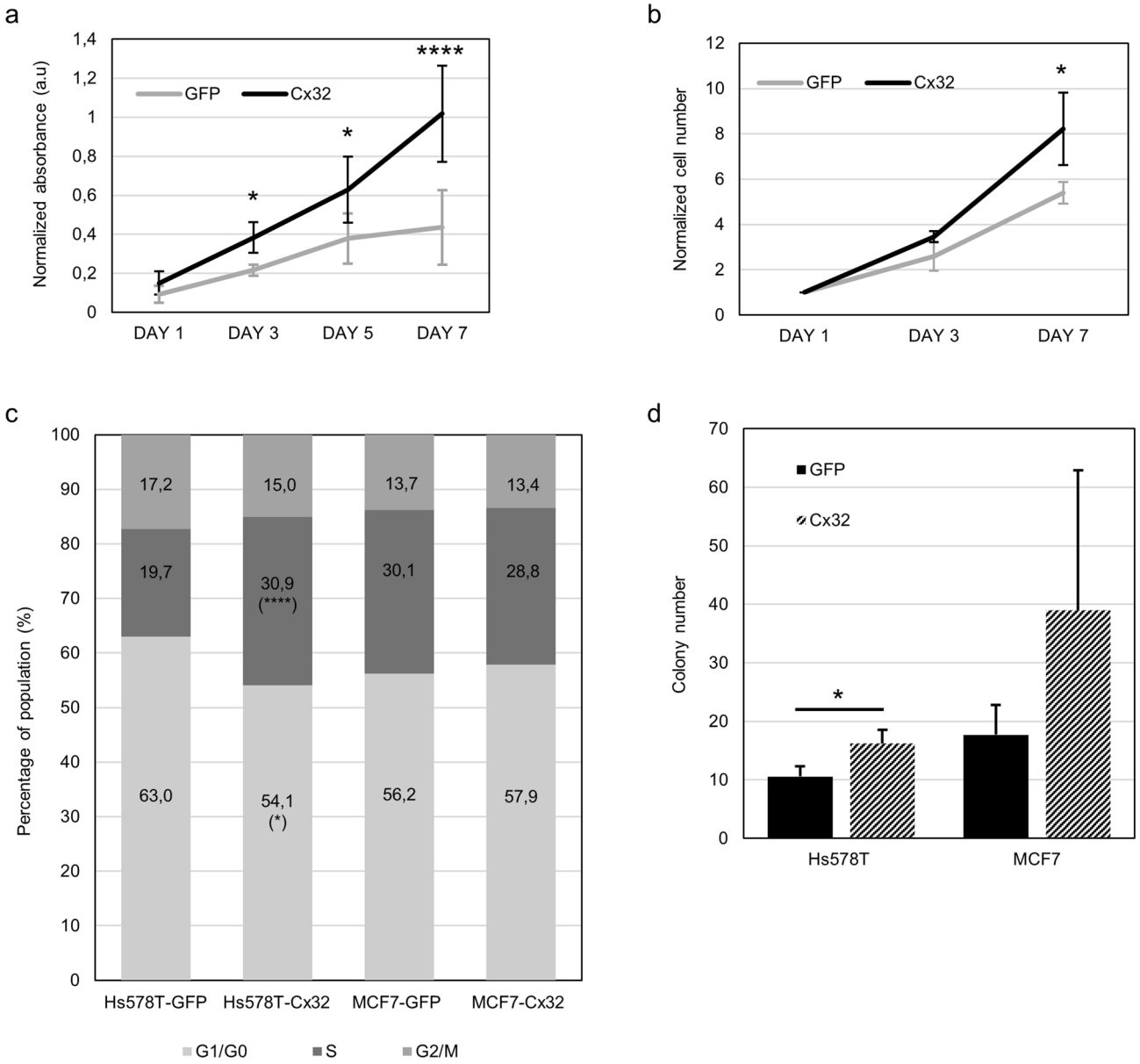

Fig. 3 Cx32 increased cell viability and proliferation in Hs578T cells. **a** MTT analysis for Hs578T cells was obtained by normalizing O.D. of Cx32 infected cells to control cells (n = 6, $*p < 0.05$, $****p < 0.001$). **b** Cell counts using trypan blue and hemocytometer in 1 ml volume normalized to day 1 for Hs578T cells (n = 9, $*p < 0.05$). **c** Cell cycle analysis of GFP and Cx32 infected cells. **d** The number of colonies in colony formation assay formed after 7 days (n = 3, $*p < 0.05$). Error bars represent S.D

with a distance of 52.8 ± 16.1 µm, overexpression of Cx32 significantly reduced the transfer distance to 41.8 ± 20.8 µm ($p < 0.001$). Treatment with CBX also significantly reduced the transfer distance to 20.8 ± 9.0 µm for Hs578T-GFP and to 19.1 ± 11.8 µm for Hs578T-Cx32 cells (Fig. 4B). In contrast, MCF7 cells did not have intercellular communication between cells so we did not observe any alteration by either Cx32 overexpression or CBX treatment (Fig. S2).

Hemichannel activity after the dye uptake assay was assessed in two ways. We first determined the number of cells that took up the dye from the extracellular environment to indicate cells with active hemichannels (Fig. S3A and S3B). For the second one, we assessed the signal intensities of the cells with active hemichannels that demonstrate the amount of activity (Fig. S3C). Dye uptake assays suggested that Hs578T-GFP and MCF7-GFP cells had negligible hemichannel activity, which was not affected by either Cx32 overexpression or the application of CBX as no difference was observed in the number of cells with fluorescent signal or the fluorescent intensity among groups (Fig. S3A–C).

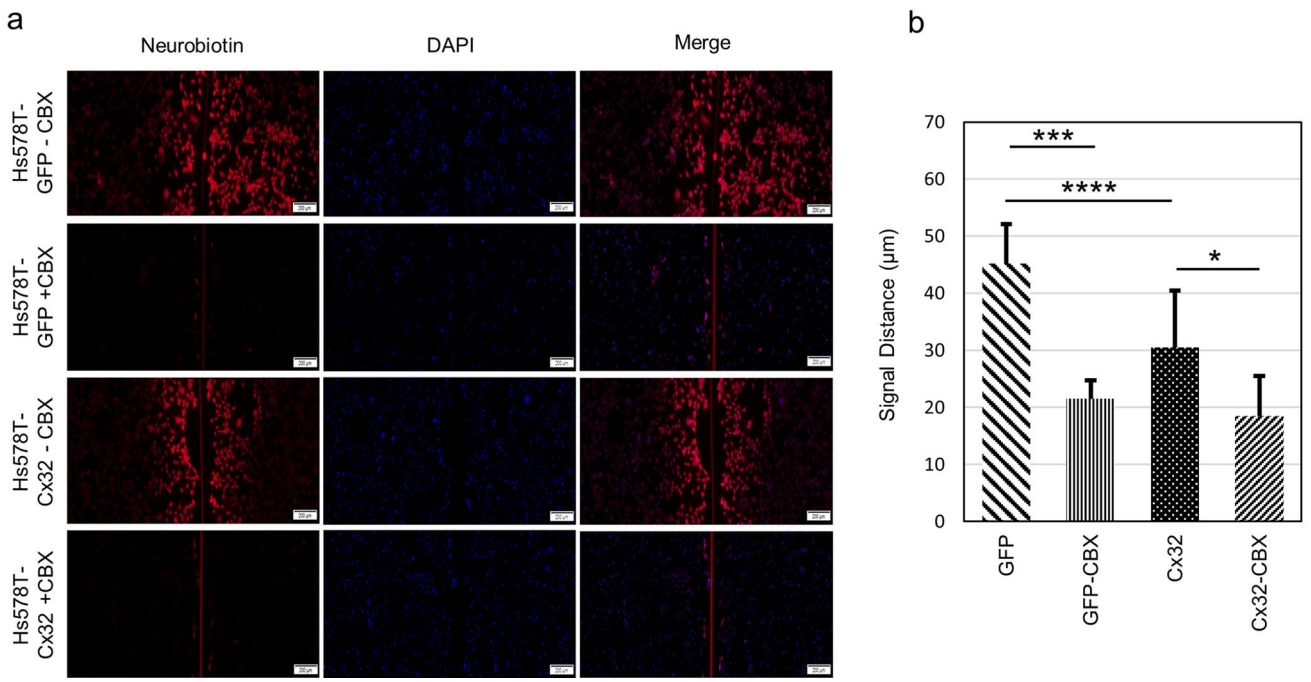

Fig. 4 Cx32 reduced gap junctional communication in Hs578T cells **a** Scrape loading of control and Cx32 infected Hs578T cells. Scale bar: 200 µm. Red is for Neurobiotin and blue is for the nucleus. **b** Comparison of the distance of the dye transfer from the site of scrape in the absence and presence of CBX in Hs578T cells (n = 4, $*p < 0.05$, $***p < 0.005$, $****p < 0.001$). Error bars represent S.D

Cx32 was mainly localized to cytoplasm in breast cancer cells

Cx32 was mainly observed in the cytosol in lymph node metastasis of breast cancer samples. Thus, the subcellular localization of Cx32 was examined by immunostaining with fluorescent microscopy in both cell types. Cx32 expression significantly increased in Hs578T-Cx32 cells compared to GFP control cells. In addition, Cx32 was mainly in the cytoplasm and no GJIC plaque was observed between cells (Fig. S4A). To further confirm the cellular location of Cx32, both untransfected and Cx32-transfected cells were co-stained with Cx32 and WGA for the plasma membrane. We did not observe colocalization between WGA and Cx32, confirming cytoplasmic localization of Cx32 in cells. In addition, Cx32 was observed to consistently localize to certain regions especially in Cx32 transfected MCF7 cells (Fig. S4B). To determine if this preferential location was the Golgi apparatus, co-staining with Cx32 and Golgin-97, a Golgi apparatus marker was performed. However, there was no colocalization between Cx32 and Golgin-97, suggesting that Cx32 did not localize to Golgi (Fig. S4C).

Cx32 resulted in reduced Cx43 expression in Hs578T cells

Observation of Cx32 in the cytoplasm and the decrease in GJIC in Hs578T with the overexpression of Cx32 suggests the potential contribution of other connexins to GJIC in these cells. For this reason, the expression and localization of two main connexins, Cx26 and Cx43 that are involved in breast homeostasis and cancer, were examined using Western blot analysis and immunostaining experiments. Cx26 protein levels did not change upon Cx32 overexpression compared to their control counterparts in either Hs578T or MCF7. On the other hand, Cx43 expression was reduced in Cx32 overexpressing Hs578T and MCF7 cells compared to GFP controls (Fig. 5A). This reduction was 68% ($p < 0.05$) in Hs578T cells and 55% ($p < 0.001$) in MCF7 cells upon Cx32 overexpression (Fig. 5B). The localization of these proteins was also examined using immunostaining analysis that demonstrated neither protein was observed at cell–cell contact areas (Fig. 5C and E). Further, Cx26 was observed in the nucleus but Cx26 localized to the cytoplasm in addition

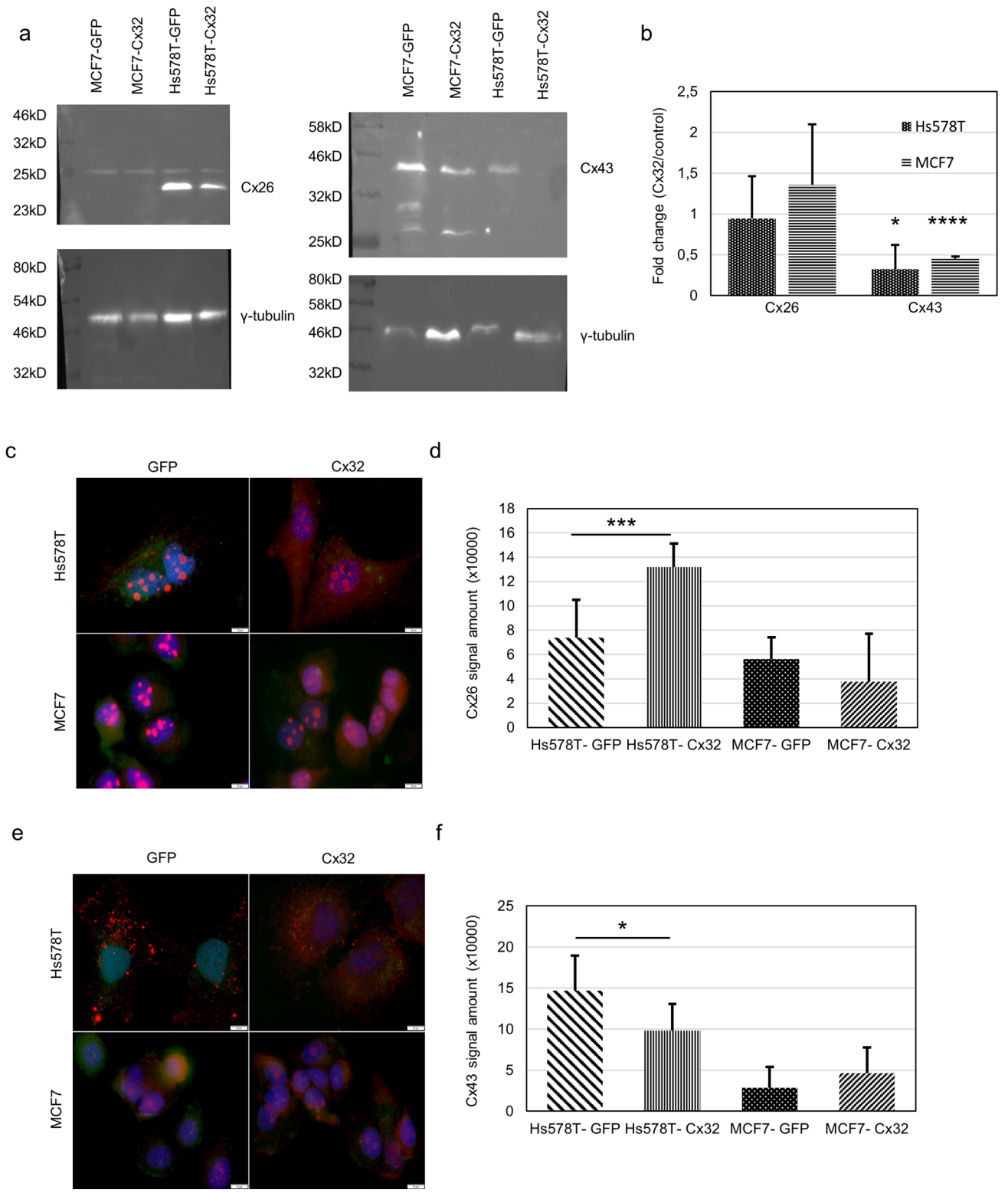

Fig. 5 Cx32 reduced the expression of Cx43 in Hs578T cells. **a** Representative images for protein levels of Cx26 and Cx43 in Hs578T and MCF7 cells. γ-tubulin was used as a loading control. **b** Quantification of Cx26 and Cx43 levels in Hs578T and MCF7 cells (n = 3, $*p < 0.05$, $****p < 0.001$). **c** Localization of Cx26 in infected cells and **d** Comparison of Cx26 signals in all cell groups. **e** Localization of Cx43 in infected cells. **f** Quantification of Cx43 signals in cells. (n = 3, $*p < 0.05$, $***p < 0.005$). Red is either for Cx26 or Cx43, green shows GFP, blue is for the nucleus in **c** and **e**. Error bars represent S.D. and the scale bar is 10 μm

to the nucleus upon Cx32 overexpression (Fig. 5C). To confirm the nuclear localization, Cx26 was assessed in the nuclear fraction of Hs578T and MCF7 after subcellular fractionation and it verified the presence of Cx26 in the nuclear extracts of both cells (Fig. S5). Additionally, when the amount of signals from the cells was analyzed, no statistically significant difference in Cx26 signals was detected in MCF7 cells, while Cx26 signal was significantly higher in Hs578T-Cx32 cells than Hs578T-GFP cells (Fig. 5D). Unlike Cx26, Cx43 was observed throughout the cytoplasm in Hs578T-Cx32 cells and the signal amounts were reduced compared to their control counterparts, confirming the Western blot analysis (Fig. 5E). Finally, no change at Cx43 signal amount between control and Cx32 infected cells was observed in MCF7 (Fig. 5F).

Both cells' migration potential and the invasion of Hs578T decreased upon Cx32 overexpression

The presence of Cx32 in cells at the lymph node metastasis of breast cancer might implicate the role of Cx32 in cellular motility or metastasis. Thus, Cx32's effects on the migration of cells were assessed using wound healing assay. Cx32 overexpression delayed the closure of the open gap 18 h after wound generation in Hs578T and MCF7 cells (Fig. 6A). The percentage of open area in Hs578T-Cx32 and MCF7-Cx32 cells increased significantly compared to GFP control cells by 3.2 folds and 1.5 folds at the 18th hour, respectively, suggesting that Cx32 decreased cells' migration potential (Fig. 6B). Moreover, the decrease in cells' migration potential became significantly different between Cx32 infected and GFP infected cells after 10 h. for Hs578T cells and after 3 h. for MCF7 cells (Fig. S6). When the velocities

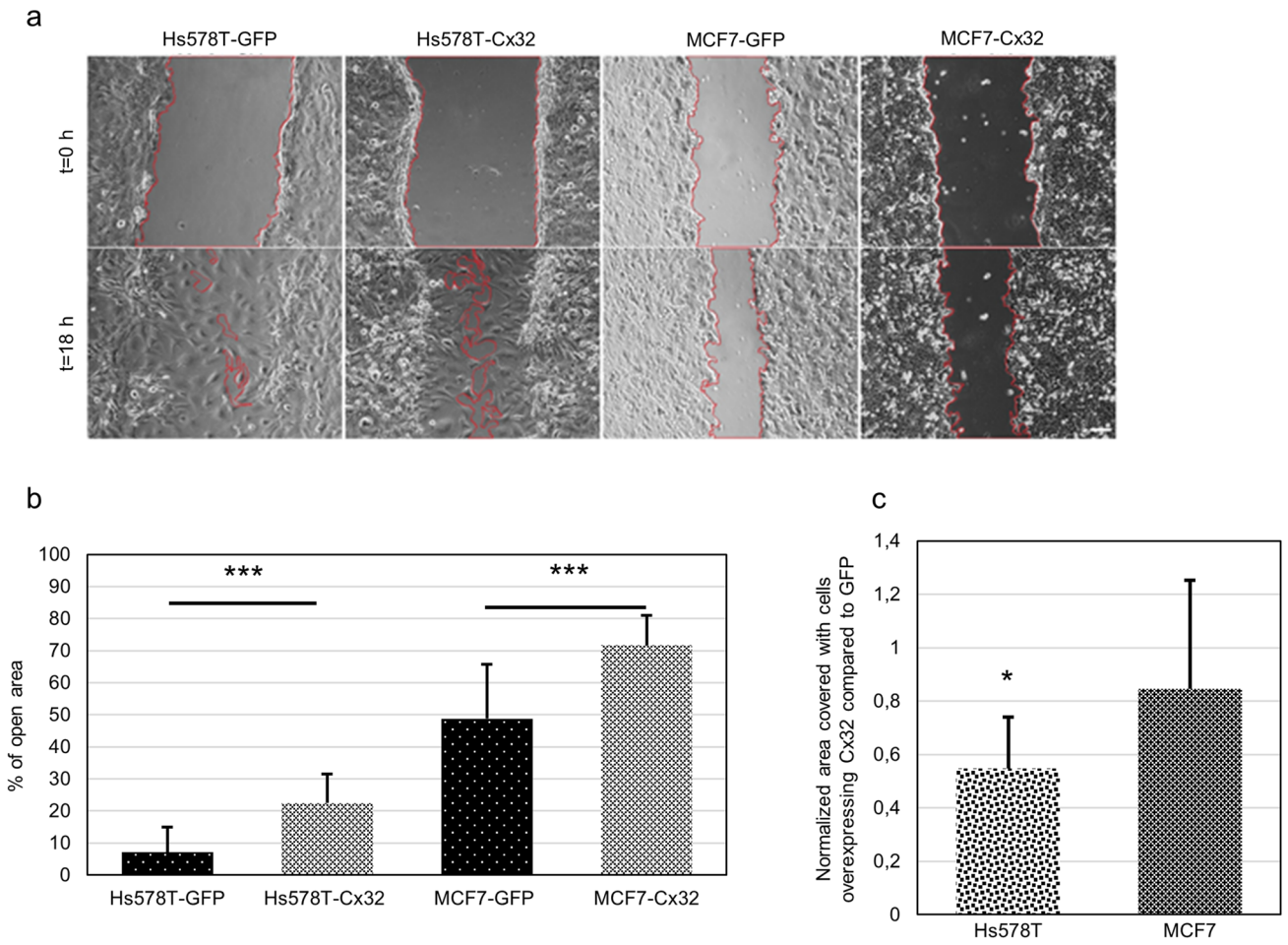

Fig. 6 Cx32 overexpression decreased migration of Hs578T and MCF7. **a** Representative images of cells taken at t = 0 h (right after the scratch) and at t = 18 h using time-lapse photography. The scale bar is 50 µm. **b** Percentages of wounds remained open after 18 h (n = 3, ***$p < 0.005$). **c** Relative area covered by invaded cells in Boyden chamber invasion assay. The graph was obtained by normalizing the area covered by the invaded Cx32 infected cells to the area covered by the invaded GFP control cells. Error bars represent S.D (n = 3, *$p < 0.05$)

of the cells were measured as percentages of the wound they cover per hour, Cx32 infection reduced migration capacity by 44% in Hs578T cells from 14.7% to 8.3% per hour and 55% in MCF7 cells from 4% to 1.8% per hour.

While migration potential is an important indicator of aggressiveness, cells need to go through the extracellular matrix by invasion before they can metastasize. To assess the ability of cells to invade, Boyden chamber invasion assay using Matrigel was used (Fig. 6C). The area covered by the invaded Hs578T-Cx32 cells was 43% less than Hs578T-GFP cells ($p < 0.05$). For MCF7 cells, MCF7-Cx32 cells had 20% less coverage compared to MCF7-GFP cells, which was not a statistically significant decrease ($p = 0.54$).

Due to the changes in migration and invasion profiles of Hs578T cells upon Cx32 overexpression, the ability of cells to go through epithelial-to-mesenchymal transition (EMT) was examined by determining the protein levels of EMT markers using Western blot analysis (Fig. 7A). Expressions

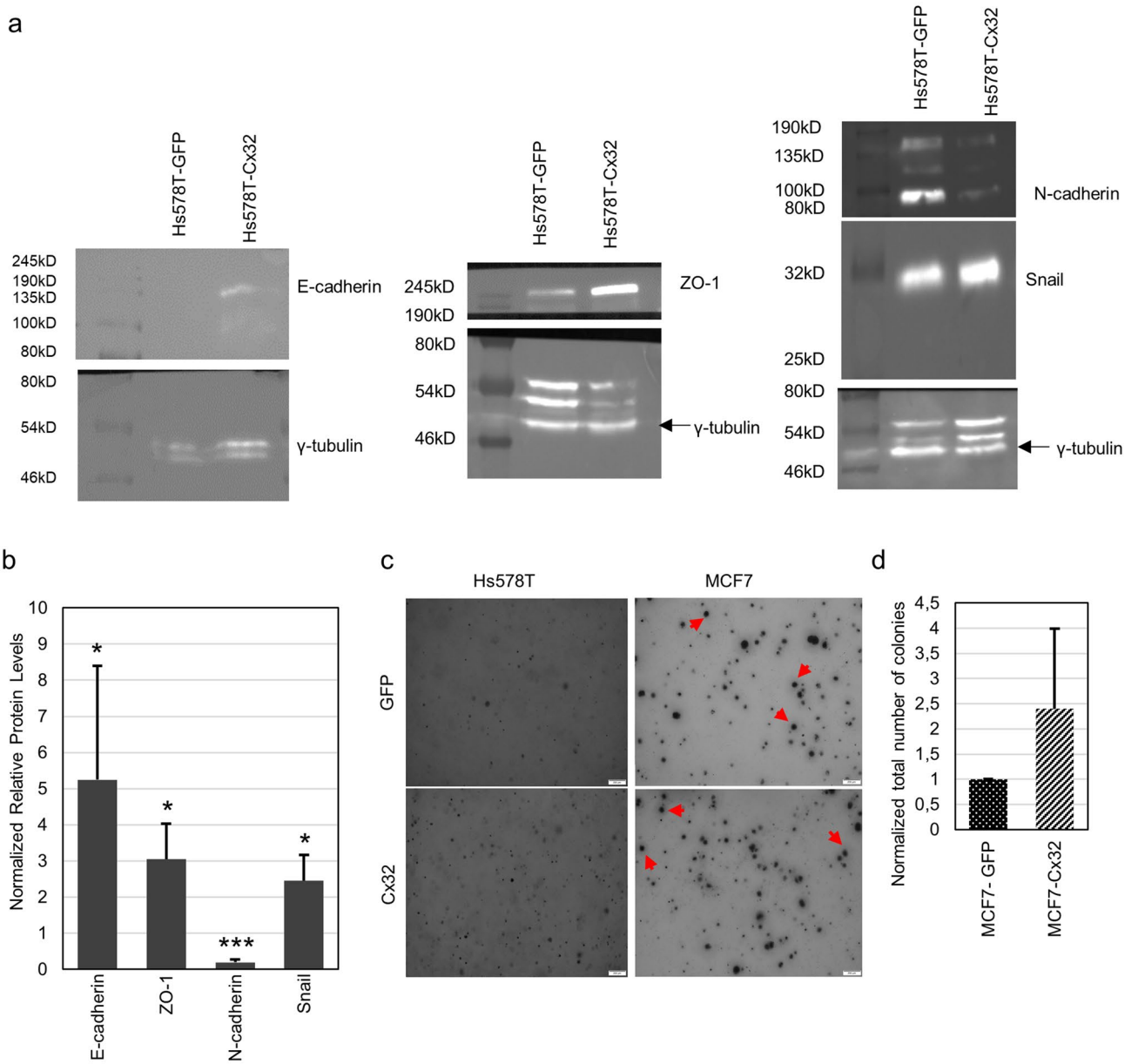

Fig. 7 Cx32 overexpression decreased EMT in Hs578T and anchorage-independent growth in MCF7 cells. **a** Representative images of Western blot of EMT markers in infected Hs578T cells. **b** Comparison of normalized protein levels for Hs578T cells (n = 3–8, *$p < 0.05$, ***$p < 0.005$). **c** Representative images of colonies for Hs578T cells after 8 weeks and MCF7 cells after 3 weeks. Red arrows show the colonies that were analyzed. **d** The relative number of colonies in MCF7 cells. The graph was obtained by normalizing colonies produced by Cx32 infected cells to control cells. Error bars represent S.D. (n = 3)

of epithelial markers E-cadherin and ZO-1 increased 5.2 folds and 3 folds in Hs578T-Cx32 cells compared to Hs578T-GFP cells, respectively. Additionally, the expression of mesenchymal transcription factor Snail (Snai1) increased 2.4 folds in Hs578T-Cx32 cells compared to Hs578T-GFP cells. On the other hand, expression of mesenchymal marker N-cadherin decreased 81% in Hs578T-Cx32 cells compared to Hs578T-GFP cells (Fig. 7B). However, expressions of these markers in MCF7 cells were not altered significantly upon Cx32 overexpression (Fig. S7).

Lastly, soft agar assay was performed to test the anchorage-independent growth to assess the effect of Cx32 on cellular transformation. Hs578T cells did not form colonies in either sample even after 8-week culture and they degraded the soft agar similar to previous reports (Mori et al. 2009; Deocesano-Pereira et al. 2019). In contrast to Hs578T cells, MCF7 cells formed adequately sized (> 30 µm in diameter) colonies after 2.5 to 3 weeks (Fig. 7C). When the colonies larger than 30 µm in diameter were counted, there were more colonies in MCF7-Cx32 cells compared to MCF7-GFP cells but this difference was not statistically significant ($p = 0.056$, Fig. 7D).

Discussion

Connexins have diverse functions in cancer based on the isoform, cell type and cancer stages. Therefore, each connexin is needed to be assessed individually to understand their roles in tumorigenesis in a context-dependent manner. In this study, we investigated the role of Cx32 in proliferation, gap junctional activity, localization and expression of other connexins in addition to aggressive features in breast cancer cells, invasive Hs578T and non-invasive MCF7. Cx32 overexpression significantly increased percentages of cells in the S phase and subsequently the proliferation of Hs578T cells with no significant change in MCF7 cells. While hemichannel activity was not observed in either cell, Cx32 overexpression reduced GJIC in Hs578T cells. In addition, Cx32 mainly localized to cytoplasm in both cells and did not form gap junctional plaques between cells. Moreover, Cx32 overexpression decreased the Cx43 level in Hs578T cells. Finally, Cx32 overexpression reduced the migration and invasion capacity of both cells in addition to causing the reduction of N-cadherin mesenchymal marker and the elevation of E-cadherin and ZO-1 epithelial markers in Hs578T cells. Overall, Cx32 overexpression had a more pronounced effect on Hs578T compared to MCF7 cells where Cx32 overexpression only altered migration and Cx43 protein levels in these cells. While Cx32 overexpression induced ~ 180-fold increase at mRNA level, its translation into protein could not be verified by Western blot in MCF7 cells. Therefore, even though the lack of significant changes in MCF7 could be attributed to cell and tissue type specific effects of Cx32, it can also be due to unaltered Cx32 protein levels upon Cx32 overexpression that already had high levels of endogenous Cx32.

Connexins are long considered to be tumor suppressors based on their inhibitory effect on the proliferation of cancer cells. However, they were also shown to have growth-promoting roles. For example, Cx43 induced proliferation in HER2(+) drug-resistant SK-BR-3 and JIMT-1 cells and Cx32 increased proliferation in response to stimuli in non-myelinating Schwann cells (NMSC), Huh7 and Li7 hepatocellular carcinoma cells (Li et al. 2007; Freidin et al. 2009; Yeh et al. 2017). We also observed that Cx32 increased proliferation in Hs578T cells with no significant effect on MCF7 cells, which might implicate cell type or cancer-stage specific role of Cx32 in Hs578T cells. Supporting the cell type-specific effects in breast cancers, Cx32 did not have any effect on the proliferation of MDA-MB-231 while reducing proliferation in MCF10A cells (Adak et al. 2020). Decrease in the percentage of cells in the G_1 phase and a subsequent increase in the percentage of cells in the S phase in Cx32 infected Hs578T cells suggested a possibility of shortened and/or accelerated G_1 phase, which was supported by a significant increase in proliferation. Previous studies have shown the effect of connexins on cell cycle where Cx37 in Rin cells and Cx43 in either U2OS or TRMP cells delayed cell cycle progression at the G_1/S checkpoint by acting through cyclins and CDKs, which ultimately decreased cell growth (Chen et al. 1995; Zhang et al. 2001; Burt et al. 2008). Contrarily, Cx43 silencing resulted in cell cycle arrest in Glomerular Mesangial cells (Zhang et al. 2006), and Cx43 was implicated in the proliferation of acute myeloid leukemia cells, while Cx32 did not have any effect (Yi et al. 2012). Meanwhile, in NMSC, Cx32 accelerated G_1-to-S-phase acting through Nrg1 (Monje et al. 2006; Li et al. 2007; Freidin et al. 2009). These studies supported connexins' isoform and cell/tissue-specific effect in cell growth and thus tumorigenesis.

The lack of hemichannel activity in Hs578T and MCF7 cells was expected as hemichannels open very infrequently and normally remain closed to prevent the uncontrolled exchange of materials between cytosol and the extracellular matrix under physiological conditions. In addition, the frequency of their opening does not interfere with their function (Contreras et al. 2003). Moreover, connexins can have channel-independent functions so observation of no alteration on hemichannel activity upon Cx32 overexpression might be due to Cx32's channel independent activity (Bond 1994; Duflot-Dancer 1997; Huang et al. 1998; Qin et al. 2003; Jiang and Gu 2005). Besides, the reduction of GJIC between Hs578T cells upon Cx32 overexpression suggests the involvement of other connexins in communication in these cells. Overexpression of connexins in cells

was generally associated with increased communication (Tittarelli et al. 2015; Liang et al. 2019). However, we did not observe gap junction plaques between cells upon Cx32 overexpression, which might point out channel-independent roles. Alternatively, their arrangements or distribution in cells might also interfere with their roles in communication rather than their protein levels. For example, ouabain enhanced GJIC by rearranging previously synthesized Cx43 subunits in MDCK cells without increasing the Cx43 protein expression and resulted in Cx43 relocalization to the membrane (Ponce et al. 2016). Yet, considering that neither endogenous nor exogenous Cx32 in MCF7 cells directly function in communication, Cx32 might not be involved in gap junctional functions in these cells at all. The decrease of GJIC in Hs578T cells upon Cx32 overexpression may suggest that Cx32 might influence communication by reducing gap junctional communication mediated by other connexins.

Both single and co-staining experiments showed that cells mostly had cytoplasmic Cx32 rather than gap junctional plaque-forming proteins. Relocalization of connexins to the cytosol was also observed in the prostate, gastric and colon cancers in vitro (Mehta 1999; Kanczuga-Koda et al. 2010; Jee et al. 2011) and breast cancers in vivo (Kanczuga-Koda et al. 2007). The redistribution of Cx32 in cells can be either due to its dispersion in the cytosol or its retention in an organelle such as Golgi or ER along the secretory pathway (Rahman 1993; Kyriakoudi et al. 2017). Cx32 in Hs578T and MCF7 did not colocalize with Golgin-97, a Golgi apparatus marker but whether it localizes to the ER remains to be determined. E-cadherin regulated the localization of connexins in MCPC, HSCC and IAR20 cells (Hernandez-Blazquez et al. 2001; Kawasaki et al. 2007; Chakraborty et al. 2010). Moreover, E-cadherin moved Cx26 and Cx43 to the cytoplasm by interacting with their cytoplasmic loops (Nambara et al. 2007). Further, Cx43 localization in adult cardiac myocytes was regulated through Rac1, which is in the downstream of N-cadherin, demonstrating the involvement of cadherins in the subcellular distribution of connexins (Matsuda et al. 2006). When the alterations in E-cadherin and N-cadherin levels upon Cx32 overexpression cells were considered, the roles of cadherins in Cx32 relocalization to the cytoplasm of Hs578T needs further assessment.

The function and/or expression of connexins can be altered depending on the need of cells/tissues. For example, Cx26 or Cx32 can compensate for each other in the case of abnormalities in either isoform during lactation (Locke et al. 2004; McLachlan et al. 2007; Banerjee 2016). Similarly, overexpression of Cx32 in HUVEC cells suppressed the expression of Cx43 (Okamoto et al. 2014). Therefore, alteration in expression of one isoform can affect the expression and/or function of other connexins (Bedner et al. 2012), so we examined the alterations in Cx26 and Cx43 levels and localization in Hs578T and MCF7 cells. Cx32 overexpression significantly decreased Cx43 expression in both cell types. Reduction of Cx43 expression may also suggest that the decrease in GJIC upon Cx32 overexpression could be completely or partially be caused by the Cx43 downregulation as Cx43 was shown to be the main connexin isoform mediating the dye transfer between Hs578T cells (Qin et al. 2002; Jiang et al. 2017). The localization pattern of Cx26 in MCF7 and Hs578T was unexpected with both cytosolic and pronounced nuclear localization. Cx26 was previously shown to be absent in MCF7 cells (Momiyama et al. 2003). However, recent studies demonstrated its presence in the cytoplasm and the plasma membrane of MCF7 cell lines with Western blot analysis (Thiagarajan et al. 2018) but its cytosolic distribution was not determined. The reason behind the conflicting results in MCF7 cells from different groups are not known however, studies showed clonal variations of MCF7 cells from different sources, resulting in phenotypic and genotypic heterogeneity concerning growth rates, signaling pathways, expression of hormone receptors and chromosome numbers (Jones et al 2000; Nugoli et al 2003). All these cells are related to the original MCF7 cell line and thus still considered as MCF7 (Kleensang et al 2016). This cellular heterogeneity might contribute to the observation of inconsistent results for Cx26 in MCF7 cells. Connexins are known to mainly localize to the plasma membrane (Harris 2001). However, they could localize to the cytosol including the ER and the Golgi apparatus due to disease-causing mutations and cancer (Mese et al. 2007; Unal et al. 2021). Further, Cx43 C-terminal was shown to localize to the nucleus (Dang X et al. 2003) and truncated Cx43-20k isoform was observed in the nucleus, regulating N-cadherin expression (Kotini et al. 2018). Similarly, Cx26 was found on the nuclear envelope where it interacts with NANOG and FAK in MDA MB 231 breast cancer cells (Thiagarajan et al. 2018). Cx26 nuclear staining pattern in Hs578T and MCF7 cells was quite different where they accumulated at specific sites in or around the nucleus. The reason for this unique distribution is not known, however further studies including the confocal microscopy might help to decipher the details of Cx26 subcellular localization and its significance for homeostasis of Hs578T and MCF7 cells.

Cancer cells appear to lose their migration potentials and invasive ability with Cx32 overexpression in the liver and cervical cancers (Yang et al. 2011; Zhao et al. 2014). This may suggest that Cx32 inhibits the cells' motility, which then might affect the metastatic potential. The decrease in mesenchymal marker N-cadherin and an increase in epithelial marker E-cadherin indicate a shift to epithelial characteristic in Hs578T with Cx32 overexpression. Similarly, overexpression of Cx32 converted EMT to mesenchymal-to-epithelial transition (MET) in doxorubicin-resistant hepatocellular carcinoma HepG2 cells (Yu et al. 2017). Furthermore, E-cadherin can also affect cells migration and invasion

capabilities. Since cells generally show similar trends for invasion, migration and EMT, the expression changes of EMT markers and decrease in migration and invasion in Hs578T cells were consistent. Similarly, in hepatocellular carcinoma cell line SMMC-7721, knockdown of Cx32 enhanced invasion and migration and lowered E-cadherin (Zhao et al. 2014). Besides, Cx32's effect on migration and invasion might be related with Cx43 expression in both cells but the changes in EMT marker expression are possibly due to Cx32 presence, as it was not observed in MCF7. The soft agar results in MCF7 cells, on the other hand, indicated that MCF7 cells showed a tendency to gain stem cell characteristics upon Cx32 overexpression. The inhibitory effects of connexins on anchorage-independent growth have been observed with Cx43 in BL6 malignant melanoma cells, in breast cancer cells MDA-MB-231 and with Cx32 in adenocarcinoma A549 and renal cell carcinoma Caki-2 cells (Fujimoto et al. 2004; McLachlan et al. 2006; Hada et al. 2006; Ableser et al. 2014).

Conclusion

Our results showed a trend that Cx32 expressing cells had different features than cells with no Cx32. The best example was observed in cell cycle analysis, where Cx32 expressing cells (uninfected MCF7 or Cx32 infected Hs578T cells) have similar percentages of cells in all phases of the cell cycle, which are significantly different from the percentages in Cx32-lacking cells (Hs578T-GFP). Apart from proliferation, it was also observed that Cx32 overexpression caused Hs578T cells to behave similar to Cx32 expressing MCF7 cells in terms of GJIC, migration and invasion. As a conclusion, Hs578T-Cx32 becomes similar to faster proliferating, slower migrating, less invading, non-communicating MCF7 cells that have endogenous Cx32. Overall, we provided further support for context-dependent functions of Cx32 in breast cancer and observed a tumor-suppressive effect of Cx32 in Hs578T breast cancer cells.

Supplementary Information The online version contains supplementary material available at https://doi.org/10.1007/s12079-021-00665-9.

Acknowledgements We thank Dr. Steven Scherer from University of Pennsylvania, PA, USA for kindly providing the pIRES2-EGFP2-Cx32 vector. The Biotechnology and Bioengineering Research and Application Center, Izmir Institute of Technology staff and Ms Yagmur Ceren Unal is gratefully acknowledged for their expert technical help.

Author contributions GM conceived the project; DU performed the majority of experiments with contribution from TBG (Cx26 and Cx43 immunostaining experiments), SY (Golgi-Cx32 co-immunostaining experiments), OYO and GM; GM, DU, OYO and EO designed the experiments; DU, EO and GM analyzed the data; GM and DU wrote the manuscript; all authors edited the manuscript.

Funding This work was supported by The Scientific and Technological Research Council of Turkey (114Z874 to GM) and Izmir Institute of Technology Research Fund (2019IYTE0235 to GM). The Young Investigator Award by the Turkish Academy of Sciences (GM) is also highly appreciated.

Data availability Data sharing is not applicable to this article as no datasets were generated or analysed during the current study.

Declarations

Conflict of interest The authors declare that they have no conflict of interest.

References

Ableser MJ, Penuela S, Lee J, Shao Q, Laird DW (2014) Connexin43 reduces melanoma growth within a keratinocyte microenvironment and during tumorigenesis in vivo. J Biol Chem 289(3):1592–1603. https://doi.org/10.1074/jbc.M113.507228

Adak A, Unal YC, Yucel S, Vural Z, Turan FB, Yalcin-Ozuysal O et al (2020) Connexin 32 induces pro-tumorigenic features in MCF10A normal breast cells and MDA-MB-231 metastatic breast cancer cells. Biochimica Et Biophysica Acta BBA - Molecular Cell Research. https://doi.org/10.1016/j.bbamcr.2020.118851

Avanzo JL, Mesnil M, Hernandez-Blazquez FJ, Mackowiak II, Mori CMC, da Silva TC et al (2004) Increased susceptibility to urethane-induced lung tumors in mice with decreased expression of connexin43. Carcinogenesis 25(10):1973–1982. https://doi.org/10.1093/carcin/bgh193

Banerjee D (2016) Connexin's connection in breast cancer growth and progression. Int J Cell Bio. https://doi.org/10.1155/2016/9025905

Bedner P, Steinhäuser C, Theis M (2012) Functional redundancy and compensation among members of gap junction protein families. Biochimica Et Biophysica Acta BBA - Biomembranes. https://doi.org/10.1016/j.bbamem.2011.10.016

Bond SL, Bechberger JF, Khoo NK, Naus CC (1994) Tranfection of C6 glioma cells with connexin32: the effects of expression of a non-endogenous gap junction protein. Cell Growth Differ 5:179–186

Brauner T, Hülser DF (1990) Tumor cell invasion and gap junctional communication II. Normal and Malignant Cells Confronted in Multieell Spheroids' Invasion Metastasis 10:31–43

Burt JM, Nelson TK, Simon AM, Fang JS (2008) Connexin 37 profoundly slows cell cycle progression in rat insulinoma cells. Am J Physiol-Cell Physiol. https://doi.org/10.1152/ajpcell.299.2008

Chakraborty S, Mitra S, Falk MM, Caplan SH, Wheelock MJ, Johnson KR et al (2010) E-cadherin differentially regulates the assembly of Connexin43 and Connexin32 into gap junctions in human squamous carcinoma cells. J Biol Chem 285(14):10761–10776

Chen SC, Pelletier DB, Peng A, Boynton AL (1995) Connexin43 reverses the phenotype of transformed cells and alters their expression of cyclin/cyclin-dependent kinases. Cell Growth Differ 6:681–690

Contreras JE, Sáez JC, Bukauskas FF, Bennett MVL (2003) Gating and regulation of connexin 43 (Cx43) hemichannels. PNAS 100(20):11388–11393. https://doi.org/10.1073/pnas.1434298100

Cronier L, Crespin S, Strale PO, Defamie N, Mesnil M (2009) Gap junctions and cancer: new functions for an old story. Antioxid Redox Signal 11(2):323–338. https://doi.org/10.1089/ars.2008.2153

Dahl G, Muller KJ (2014) Innexin and pannexin channels and their signaling. FEBS Lett 588(8):1396–1402. https://doi.org/10.1016/j.febslet.2014.03.007

Dang X, Doble BW, Kardami E (2003) The carboxy-tail of connexin-43 localizes to the nucleus and inhibits cell growth. Mol Cell Biochem 242(1–2):35–38

Deocesano-Pereira C, Machado RAC, De Jesus-Ferreira HC, Marchini T, Pereira TF, Carreira ACO et al (2019) Functional impact of the long non-coding RNA MEG3 deletion by CRISPR/Cas9 in the human triple negative metastatic Hs578T cancer cell line. Oncol Lett 18(6):5941–5951. https://doi.org/10.3892/ol.2019.10969

Duflot-Dancer AM, Mesnil M, Yamasaki H (1997) Dominant-negative abrogation of connexin-mediated cell growth control by mutant connexin genes. Oncogene 18:2151–2158

Eghbali B, Kessler JA, Reid LM, Roy C, Spray DC (1991) Involvement of gap junctions in tumorigenesis: transfection of tumor cells with connexin 32 cDNA retards growth in vivo. Proc Natl Acad Sci U S A 88(23):10701–10705. https://doi.org/10.1073/pnas.88.23.10701

Freidin M, Asche S, Bargiello TA, Bennett MV, Abrams CK (2009) Connexin 32 increases the proliferative response of Schwann cells to neuregulin-1 (Nrg1). Proc Natl Acad Sci U S A 106(9):3567–3572. https://doi.org/10.1073/pnas.0813413106

Fujimoto E, Satoh H, Negishi E, Ueno K, Nagashima Y, Hagiwara K et al (2004) Negative growth control of renal cell carcinoma cell by connexin 32: possible involvement of Her-2. Mol Carcinog 40(3):135–142. https://doi.org/10.1002/mc.20025

Graeber SH, Hülser DF (1998) Connexin transfection induces invasive properties in HeLa cells. Exp Cell Res 243(1):142–149. https://doi.org/10.1006/excr.1998.4130

Hada S, Sato H, Virgona N, Hagiwara H, Saito T, Suzuki K et al (2006) Connexin 32 expression reduces malignant phenotype in human A549 adenocarcinoma cells: Implication of Src involvement. Oncol Rep 16(5):1149–1154. https://doi.org/10.3892/or.16.5.1149

Harris AL (2001) Emerging issues of connexin channels: biophysics fills the gap. Q Rev Biophys 34(3):325–472. https://doi.org/10.1017/s0033583501003705

Hernandez-Blazquez FJ, Joazeiro PP, Omori Y, Yamasaki H (2001) Control of intracellular movement of connexins by E-cadherin in murine skin papilloma cells. Exp Cell Res 270(2):235–247. https://doi.org/10.1006/excr.2001.5342

Hirschi K, Xu C, Tsukamoto T, Sager R (1996) Gap junction genes Cx26 and Cx43 individually suppress the cancer phenotype of human mammary carcinoma cells and restore differentiation potential. Cell Growth Differ 7(7):861–870

Huang R-P, Fan Y, Hossain MZ, Peng A, Zeng Z-L, Boynton AL (1998) Reversion of the neoplastic phenotype of human glioblastoma cells by connexin 43 (cx43). Can Res 58(22):5089–5096

Ito A, Katoh F, Kataoka TR, Okada M, Tsubota N, Asada H et al (2000) A role for heterologous gap junctions between melanoma and endothelial cells in metastasis. J Clin Investig 105(9):1189–1197. https://doi.org/10.1172/JCI8257

Ito A, Koma Y-i, Uchino K, Okada T, Ohbayashi C, Tsubota N et al (2006) Increased expression of connexin 26 in the invasive component of lung squamous cell carcinoma: Significant correlation with poor prognosis. Cancer Lett 234(2):239–248. https://doi.org/10.1016/j.canlet.2005.03.049

Jee H, Nam KT, Kwon H-J, Han S-U, Kim D-Y (2011) Altered expression and localization of connexin32 in human and murine gastric carcinogenesis. Dig Dis Sci 56(5):1323–1332. https://doi.org/10.1007/s10620-010-1467-z

Jee H, Lee S-H, Park J-W, Lee B-R, Nam KT, Kim D-Y (2013) Connexin32 inhibits gastric carcinogenesis through cell cycle arrest and altered expression of p21Cip1and p27Kip1. BMB Rep 46(1):25–30. https://doi.org/10.5483/bmbrep.2013.46.1.078

Jiang JX, Gu S (2005) Gap junction- and hemichannel-independent actions of connexins. Biochimica Et Biophysica Acta (BBA) - Biomembranes. 1711(2):208–214

Jiang G, Dong S, Yu M, Han X, Zheng C, Zhu X et al (2017) Influence of gap junction intercellular communication composed of connexin 43 on the antineoplastic effect of adriamycin in breast cancer cells. Oncol Lett 13(2):857–866. https://doi.org/10.3892/ol.2016.5471

Jin X, Mu P (2005) Targeting breast cancer metastasis. Breast Cancer (auckl) 9(Suppl 1):23–34. https://doi.org/10.4137/BCBCR.S25460

Jones C, Payne J, Wells D, Delhanty JD, Lakhani SR, Kortenkamp A (2000) Comparative genomic hybridization reveals extensive variation among different MCF-7 cell stocks. Cancer Genet Cytogenet 117(2):153–158. https://doi.org/10.1016/s0165-4608(99)00158-2

Kanczuga-Koda L, Sulkowski S, Lenczewski A, Koda M, Wincewicz A, Baltaziak M et al (2006) Increased expression of connexins 26 and 43 in lymph node metastases of breast cancer. J Clin Pathol 59(4):429–433

Kanczuga-Koda L, Sulkowska M, Koda M, Rutkowski R, Sulkowski S (2007) Increased expression of gap junction protein–connexin 32 in lymph node metastases of human ductal breast cancer. Folia Histochem Cytobiol 45(I):175–180

Kanczuga-Koda L, Koda M, Sulkowski S, Wincewicz A, Zalewski B, Sulkowska M (2010) Gradual loss of functional gap junction within progression of colorectal cancer—a shift from membranous CX32 and CX43 expression to cytoplasmic pattern during colorectal carcinogenesis. In Vivo 24(1):101–107

Kawasaki Y, Kubomoto A, Yamasaki H (2007) Control of intracellular localization and function of Cx43 by SEMA3F. J Membr Biol 217(1–3):53–61. https://doi.org/10.1007/s00232-007-9051-y

Kleensang A, Vantangoli M, Odwin-DaCosta S et al (2016) Genetic variability in a frozen batch of MCF-7 cells invisible in routine authentication affecting cell function. Sci Rep 6:28994. https://doi.org/10.1038/srep28994

Kotini M, Barriga EH, Leslie J, Gentzel M, Rauschenberger V, Schambon A, Mayor R (2018) Gap junction protein Connexin-43 is a direct transcriptional regulator of N-cadherin in vivo. Nat Commun. https://doi.org/10.1038/s41467-018-06368-x

Kyriakoudi S, Sargiannidou I, Kagiava A, Olympiou M, Kleopa KA (2017) Golgi-retained Cx32 mutants interfere with gene addition therapy for CMT1X. Hum Mol Genet 26(9):1622–1633. https://doi.org/10.1093/hmg/ddx064

Li Q, Omori Y, Nishikawa Y, Yoshioka T, Yamamoto Y, Enomoto K (2007) Cytoplasmic accumulation of connexin32 protein enhances motility and metastatic ability of human hepatoma cells in vitro and in vivo. Int J Cancer 121(3):536–546. https://doi.org/10.1002/ijc.22696

Liang J, Chen P, Li C, Li D, Wang J, Xue R et al (2019) IL-22 Downregulates Cx43 expression and decreases gap junctional intercellular communication by activating the JNK pathway in psoriasis. J Invest Dermatol 139(2):400–411

Locke D, Stein T, Davies C, Morris J, Harris AL, Evans WH et al (2004) Altered permeability and modulatory character of connexin channels during mammary gland development. Exp Cell Res 298(2):643–660. https://doi.org/10.1016/j.yexcr.2004.05.003

Matsuda T, Fujio Y, Nariai T, Ito T, Yamane M, Takatani T et al (2006) N-cadherin signals through Rac1 determine the localization of connexin 43 in cardiac myocytes. J Mol Cell Cardiol 40(4):495–502. https://doi.org/10.1016/j.yjmcc.2005.12.010

McLachlan E, Shao Q, Wang H, Langlois S, Laird DW (2006) Connexins act as tumor suppressors in three-dimensional mammary cell organoids by regulating differentiation and angiogenesis. Can Res 66(20):9886–9894. https://doi.org/10.1158/0008-5472.CAN-05-4302

McLachlan E, Shao Q, Laird DW (2007) Connexins and gap junctions in mammary gland development and breast cancer progression. J Membr Biol 218(1–3):107–121. https://doi.org/10.1007/s00232-007-9052-x

Mehta PP, Perez-Stable C, Nadji M, Mian M, Asotra K, Roos BA (1999) Suppression of human prostate cancer cell growth by

forced expression of connexin genes. Dev Genet 24:91–110. https://doi.org/10.1002/(SICI)1520-6408(1999)24:1/2<91::AID-DVG10>3.0.CO;2-#.
Meşe G, Richard G, White TW (2007) Gap junctions: basic structure and function. J Invest Dermatol 127(11):2516–2524. https://doi.org/10.1038/sj.jid.5700770
Momiyama M, Omori Y, Ishizaki Y, Nishikawa Y, Tokairin T, Ogawa J, Enomoto K (2003) Connexin26-mediated gap junctional communication reverses the malignant phenotype of MCF-7 breast cancer cells. Cancer Sci 94(6):501–507. https://doi.org/10.1111/j.1349-7006.2003.tb01473.x
Monaghan P, Clarke C, Perusinghe NP, Moss DW, Chen X-Y, Evans WH (1996) Gap junction distribution and connexin expression in human breast. Exp Cell Res 223(1):29–38
Monje PV, Bartlett Bunge M, Wood PM (2006) Cyclic AMP synergistically enhances neuregulin-dependent ERK and Akt activation and cell cycle progression in Schwann cells. Glia 53(6):649–659. https://doi.org/10.1002/glia.20330
Mori S, Chang JT, Andrechek ER, Matsumura N, Baba T, Yao G et al (2009) Anchorage-independent cell growth signature identifies tumors with metastatic potential. Oncogene 28(31):2796–2805. https://doi.org/10.1038/onc.2009.139
Nambara C, Kawasaki Y, Yamasaki H (2007) Role of the cytoplasmic loop domain of Cx43 in its intracellular localization and function: possible interaction with cadherin. J Membr Biol 217(1–3):63–69
Nugoli M, Chuchana P, Vendrell J, Orsetti B, Ursule L, Nguyen C et al (2003) Genetic variability in MCF-7 sublines: evidence of rapid genomic and RNA expression profile modifications. BMC Cancer 3:13. https://doi.org/10.1186/1471-2407-3-13
Okamoto T, Akita N, Kawamoto E, Hayashi T, Suzuki K, Shimaoka M (2014) Endothelial connexin32 enhances angiogenesis by positively regulating tube formation and cell migration. Exp Cell Res 321(2):133–141. https://doi.org/10.3390/cancers11020237
Paul DL (1995) New functions for gap junctions. Curr Opin Cell Biol 7(5):665–672. https://doi.org/10.1016/0955-0674(95)80108-1
Ponce A, Larre I, Castillo A, Flores-Maldonado C, Verdejo-Torres O, Contreras RG et al (2016) Ouabain Modulates the Distribution of Connexin 43 in Epithelial Cells. Cell Physiol Biochem 39(4):1329–1338. https://doi.org/10.1159/000447837
Qin H, Shao Q, Curtis H, Galipeau J, Belliveau DJ, Wang T et al (2002) Retroviral delivery of connexin genes to human breast tumor cells inhibits in vivo tumor growth by a mechanism that is independent of significant gap junctional intercellular communication. J Biol Chem. https://doi.org/10.1074/jbc.M200797200
Qin H, Shao Q, Thomas T, Kalra J, Alaoui-Jamali MAL, D.W, (2003) Connexin26 regulates the expression of angiogenesis-related genes in human breast tumor cells by both GJIC-dependent and -independent mechanisms. Cell Commun Adhes 10(4–6):387–393. https://doi.org/10.1080/cac.10.4-6.387.393
Rahman S, Carlile G, Evans WH (1993) Assembly of hepatic gap junctions: topography and distribution of connexin 32 in intracellular and plasma membranes determined using sequence-specific antibodies. J Biol Chem 268:1260–1265
Saez JC, Berthoud VM, Branes MC, Martinez AD, Beyer EC (2003) Plasma membrane channels formed by connexins: their regulation and functions. Physiol Rev. https://doi.org/10.1152/physrev.00007.2003
Sánchez-Alvarez R, Paíno T, Herrero-González S, Medina JM, Tabernero A (2006) Tolbutamide reduces glioma cell proliferation by increasing connexin43, which promotes the up-regulation of p21 and p27 and subsequent changes in retinoblastoma phosphorylation. Glia 54(2):125–134
Siegel RL, Miller KD, Jemal A (2020) Cancer statistics. CA Cancer J Clin 70(1):7–30. https://doi.org/10.3322/caac.21590
Sohl GW (2004) Gap junctions and the connexin protein family. Cardiovasc Res 62(2):228–232
Teleki I, Szasz AM, Maros ME, Gyorffy B, Kulka J, Meggyeshazi N et al (2014) Correlations of differentially expressed gap junction connexins Cx26, Cx30, Cx32, Cx43 and Cx46 with breast cancer progression and prognosis. PLoS ONE 9(11):e112541. https://doi.org/10.1371/journal.pone.0112541
Thiagarajan PS, Sinyuk M, Turaga SM et al (2018) Cx26 drives self-renewal in triple-negative breast cancer via interaction with NANOG and focal adhesion kinase. Nat Commun 9:578. https://doi.org/10.1038/s41467-018-02938-1
Tittarelli A, Guerrero I, Tempio F, Gleisner MA, Avalos I, Sabanegh S et al (2015) Overexpression of connexin 43 reduces melanoma proliferative and metastatic capacity. Br J Cancer 113(2):259–267. https://doi.org/10.1038/bjc.2015.162
Unal YC, Yavuz B, Ozcivici E, Mese G (2021) The role of connexins in breast cancer: from misregulated cell communication to aberrant intracellular signaling. Tissue Barriers 6:1962698. https://doi.org/10.1080/21688370.2021.1962698
Weigelt B, Peterse JL, van't Veer LJ (2005) Breast cancer metastasis: markers and models. Nat Rev Cancer 5(8):591–602
Willecke K, Eiberger J, Degen J, Eckardt D, Romualdi A, Güldenagel M et al (2002) Structural and functional diversity of connexin genes in the mouse and human genome. Biol Chem 383(5):725–737. https://doi.org/10.1515/BC.2002.076
Yamasaki H, Krutovskikh V, Mesnil M, Tanaka T, Zaidan-Dagli ML, Omori Y (1999) Role of connexin (gap junction) genes in cell growth control and carcinogenesis. Comptes Rendus De L'académie Des Sciences-Series III-Sciences De La Vie 322(2):151–159. https://doi.org/10.1016/s0764-4469(99)80038-9
Yang J, Liu B, Wang Q, Yuan D, Hong X, Yang Y et al (2011) Connexin 32 and its derived homotypic gap junctional intercellular communication inhibit the migration and invasion of transfected HeLa cells via enhancement of intercellular adhesion. Mol Med Rep 4(5):971–979. https://doi.org/10.3892/mmr.2011.509
Yeh ES, Williams CJ, Williams CB, Bonilla IV, Klauber-DeMore N, Phillips SL (2017) Dysregulated connexin 43 in HER2-positive drug resistant breast cancer cells enhances proliferation and migration. Oncotarget 8(65):109358–109369
Yi S, Chen Y, Wen L, Yang L, Cui G (2012) Expression of connexin 32 and connexin 43 in acute myeloid leukemia and their roles in proliferation. Oncol Lett 4(5):1003–1007. https://doi.org/10.3892/ol.2012.884
Yu M, Han G, Qi B, Wu X (2017) Cx32 reverses epithelial-mesenchymal transition in doxorubicin-resistant hepatocellular carcinoma. Oncol Rep 37(4):2121–2128. https://doi.org/10.3892/or.2017.5462
Zhang Y-W, Morita I, Ikeda M, Ma K-W, Murota S (2001) Connexin43 suppresses proliferation of osteosarcoma U2OS cells through post-transcriptional regulation of p27. Oncogene. https://doi.org/10.1038/sj.onc.1204563
Zhang X, Chen X, Wu D, Liu W, Wang J, Feng Z et al (2006) Down-regulation of connexin 43 expression by high glucose induces senescence in glomerular mesangial cells. J Am Soc Nephrol 17(6):1532–1542. https://doi.org/10.1681/ASN.2005070776
Zhao B, Zhao W, Wang Y, Zhang S, Yin Z, Wu Q et al (2014) Connexin32 regulates hepatoma cell metastasis and proliferation via the p53 and Akt pathways. Oncotarge 6(12):10116–10133